12th AIAA/ISSMO Multidisciplinary Analysis and Optimization Conference
September 10–12, 2008, Victoria, British Columbia, Canada

Aerostructural Shape Optimization of Wind Turbine Blades Considering Site-Specific Winds

Gaetan Kenway*, Joaquim R. R. A. Martins†
University of Toronto Institute for Aerospace Studies
Toronto, Ontario, Canada, M3H 5T6

The global installed capacity of wind energy has been increasing steadily over the past decade, and the price of electricity derived from it has been continuously declining. While viable siting locations with with high quality wind resources still exist, improved turbine technology and cost reductions can expand the number of locations that are economically viable. This paper investigates the multidisciplinary nature of wind turbine design as it applies to turbine blades. The goal is to reduce the end unit cost of electricity, amortized over the turbine lifetime, for a particular location. A multidisciplinary design feasible (MDF) approach is used for solving the optimization problem. The blade aerostructural analysis couples a quasi-3D aerodynamic analysis — performed using a blade element momentum theory (BEM) method — with a six degree of freedom beam finite element model of the internal spar. Sensitivities for both the aerodynamic and structural analysis are computed using the complex step method. Finally, multipoint optimization of a small 5.0kW fixed pitch "urban" wind turbine is performed based on the local wind velocity histograms.

I. Introduction

With the world experiencing another era of elevated oil prices, much attention has been focused on alternative sources of energy. Additional concerns over the effect of green house gases have resulted in more attention on renewable sources with no carbon emissions, such as wind energy.

Despite the fact wind energy suffers from the variable nature of the weather, significant portions of some country's electricity needs can be provided by the wind. The Dutch experience has shown that wind energy can contribute up to 20% without significant changes to existing infrastructure. With significant improvements in wind turbine technology, along with a reduction in the associated costs, the overall cost of energy for wind turbines is becoming competitive with more traditional sources.

While the theoretical maximum power available to a wind turbine is governed by the Betz's limit, improvement can still be made towards this ideal. The main goal of this project is to investigate how wind turbine blades can be optimized to maximize the potential for a particular local wind resource. Fuglsang et. al[1] conducted an extensive project into the site-specific optimization of turbines. Several characteristic siting locations are considered as well as possible optimization scenerios. Most general aspects of turbine design are considered including tower design, drivetrain components and rotor design. With a cost model the cost of energy was optimized. The authors report for onshore wind farms and redesigning a subset of major components, reductions in the cost of energy range from 0% to 8%. Cost minimization for large turbines considering the layout and localized wind velocities for a fixed turbine design was carried out by Fuglsang.[2] Wind turbine optimization has been investiged by numerous authors,[3–5] however, to the authors' knowledge, no previous work has integrated the optimization of blade airfoils into the site-specific rotor optimization problem.

*Ph.D. Candidate, AIAA Student Member
†Associate Professor, AIAA Senior Member

The wind turbine analysis in the present work is an in-house blade element-momentum (BEM) theory formulation. The formulation is extended by integrating it with XFOIL[6] to account for changes in the airfoil thickness properties of the blade. XFOIL calculates lift, drag and moment coefficients in response to changes in blade shape, chord, twist, and Reynolds number. The structure of the blade is modelled using an equivalent beam model of the spar with an in-house code, pyFEA.

This paper describes the aerodynamic, structural and multidisciplinary tools used in the analysis of wind turbines. The optimization problem being investigated is discussed followed by the results and conclusions.

II. Methodology

A. Aerodynamic Analysis

1. *Blade Element Momentum Method*

The blade element momentum (BEM) theory method is well-known and has been widely used. BEM is an extension of simple 1D momentum theory. The low computational cost and the relativity good accuracy has led to its widespread use in the wind turbine industry, both for design analysis and design optimization. The majority of BEM codes are fairly similar, differing primarily in their nonlinear solution strategy and semi-empirical correction factors to correct for effects not explicitly accounted for in the model. An in-house BEM code, pyBEM, was developed for the current project. The analysis portion of the code is written in Fortran 90, wrapped using `f2py`,[7] while the remainder of the program input, control and output are written in Python. The BEM model is as described by Hansen.[8] However, since we are interested in exploiting aerostructural coupling, the BEM method is extended to model coned rotors. While explicitly designing for pre-coned rotors is possible, here we are only interested in modelling the effect of the blade deflections on the power output. In this work, the conning is handled using the methodology of Mikkelsen[9]

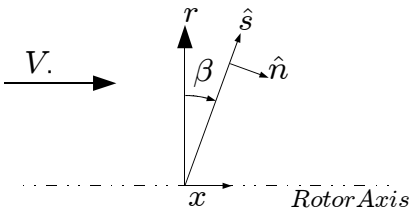

Figure 1. Coning rotor

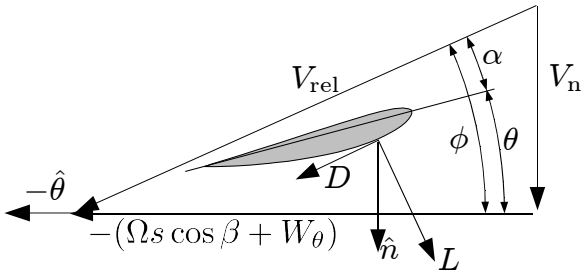

Figure 2. Velocities at blade section s. Angles are with respect to the plane of the rotor

Figure 1 shows a rotor coned at an angle β in the (x, r) plane. We consider the local coordinate system where $\hat{s}$ is along the spanwise direction of the blade and $\hat{n}$ is perpendicular to the blade. The velocity normal to the blade, assuming an induced normal velocity W_n calculated by the BEM method, is given by

$$V_n = V_0 \cos\beta - W_n - V_r \sin\beta \tag{1}$$

Since BEM methods cannot model spanwise flow, the last term must be neglected. Note that since $\cos\beta = \cos(-\beta)$ this method cannot distinguish between upwind and downwind coning. A given slice of a turbine blade at a radial distance s experiences the velocities shown in Figure 2. Ω is the rotational rate and W_θ is the induced tangential velocity. We can now find the angle ϕ using

$$\phi = \tan^{-1}\left(\frac{V_n}{\Omega s \cos\beta + W_\theta}\right). \tag{2}$$

The angle of attack is then given by

$$\alpha = \phi - \theta \tag{3}$$

. We can also compute the effective local velocity from

$$V_{\text{rel}} = \sqrt{V_n^2 + (\Omega s \cos\beta + W_\theta)^2}. \tag{4}$$

The local Reynolds number is

$$Re = \frac{\rho V_{\text{rel}} c}{\mu}, \tag{5}$$

where ρ is the air density, c is the local chord, and μ is the fluid viscosity. It is now possible to calculate the lift, drag and moment forces per unit length for each section. These forces are decomposed into the normal and tangential directions as follows

$$F_{\text{n}} = L\cos\phi + D\sin\phi, \qquad F_\theta = L\sin\phi - D\cos\phi \tag{6}$$

These forces can finally be transformed to the axial and radial components.

$$F_x = F_n\cos\beta, \qquad F_r = F_n\sin\beta. \tag{7}$$

A Glauert correction factor, as well as a Prandtl tip and hub loss correction factor are applied to the equations. The solution is obtained using a fixed point iteration scheme until both the axial and tangential induction factors converge to within a specified tolerance. Once the aerodynamic analysis is converged, postprocessing can be used to calculate the applicable loads. By construction, all structural nodes and blade element analysis positions are coincident, which simplifies the load transfer. We assume a linear load distribution between computation stations to calculate the nodal loading on the structural mesh. This transfer is formulated to be consistant and conservative, such that the work done by the forces and moments are equal in both meshes.

2. XFOIL

XFOIL is a well-known 2D panel method solver with a viscous formulation. It can be used to efficiently estimate lift-to-drag ratios of isolated 2D airfoils at low Reynolds numbers. XFOIL version 6.94 is utilized in this work, with all the GUI and plotting routines removed. It is then wrapped with `f2py`,[7] which enables direct memory access from Python. For the optimization results presented, XFOIL is used to pre-compute the lift, drag and moment coefficients for airfoils in the NACA 44XX series. Airfoil designations ranging from 4406 to 4420 are computed. This data is then stored and is available to the BEM code via three-dimensional tensor cubic B-spline interpolation.[10] The three variables are: angle of attack, Reynolds number, and airfoil thickness. Cubic polynomial basis functions are used since they ensure the C_1 continuity required for gradient based optimization. Two computed maps are shown in Figures 3 and 4.

3. Post-Stall Extrapolation of Coefficients

Stall regulated turbines use the reduction in aerodynamic lift and increase in drag that occurs post stall to control the amount of power extracted from the wind. This requires, however, 2D aerodynamic data in the post stall regime. This data can be difficult to calculate accurately using even the most advanced methods. The simple extrapolation method described by Tangler[11] is used here. The model essentially blends the pre-stall with post-stall data that is consistent with that of a flat plate in the limit where the angle of attach approaches $\pm 90°$. Equations (8– 14) describe the application of this method.

A separate approach is used to extrapolate the moment coefficients beyond the stall range. Montgomerie[12] uses the position of the center of pressure, x_{cp}, to compute the moment coefficient using

$$C_m = (-C_{\text{L}}\cos(\alpha) - C_{\text{D}}\sin(\alpha))(x_{cp} - 0.25) \tag{15}$$

. In the limit, as α approaches $\pm 90°$, we can immediately see the center of pressure must approach 0.5 in both cases as we expect a pure drag force acting at the $0.5c$ position. By linearly interpolating the arm calculation between the stall angle, α_{stall}, and this limiting value, we can then determine the moment coefficient computed at the 1/4 chord position for all angles from -90°to 90°.

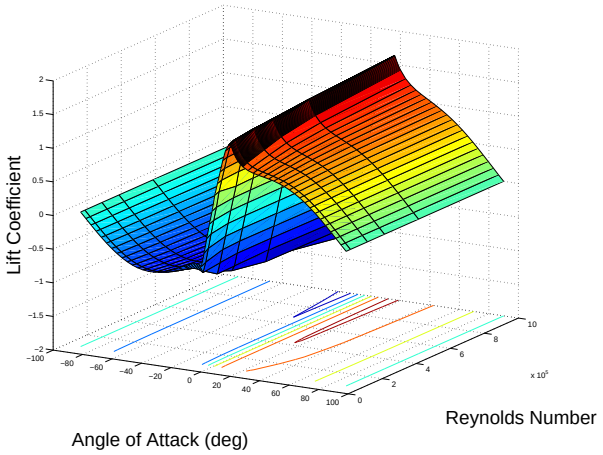

Figure 3. NACA 4415 C_L map

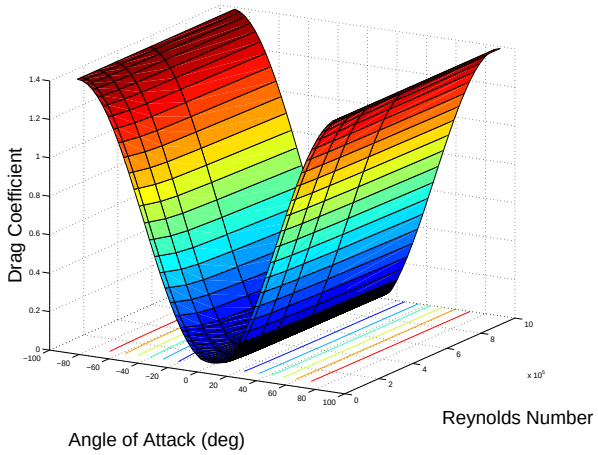

Figure 4. NACA 4415 C_D map

$$C_{d_{\max}} = 1.11 + 0.018\text{AR} \quad (\alpha = 90^{\text{o}}) \tag{8}$$

$$C_d = B_1 \sin\alpha + B_2 \cos\alpha \quad (\alpha > \alpha_{\text{stall}}) \tag{9}$$

$$B_1 = C_{d_{\max}} \tag{10}$$

$$B_2 = \frac{C_{d_{\text{stall}}} - C_{d_{\text{stall}}} \sin^2 \alpha_{\text{stall}}}{\cos \alpha_{\text{stall}}} \tag{11}$$

$$C_l = A_1 \sin 2\alpha + A_2 \frac{\cos^2 \alpha}{\sin \alpha} \quad (\alpha > \alpha_{\text{stall}}) \tag{12}$$

$$A_1 = \frac{B_1}{2} \tag{13}$$

$$A_2 = (C_{l_{\text{stall}}} - C_{d_{\max}} \sin \alpha_{\text{stall}} \cos \alpha_{\text{stall}}) \frac{\sin \alpha_{\text{stall}}}{\cos^2 \alpha_{\text{stall}}} \tag{14}$$

B. Structural Analysis

Since the analysis of wind turbine blades is an inherently multidisciplinary problem, a structural analysis model must be included to account for the deformation that results from aerodynamic loading. We assume quasi-steady aerostructural solutions. A single equivalent beam model with six degree of freedom Timoshenko elements is utilized. This structures program, pyFEA, is implemented entirely in Python. The structural analysis is somewhat less complex than the aerodynamic analysis, since the stiffness matrix needs to be generated once only. The factorization of this matrix is stored, and then all subsequent structural analysis for a given set of design variables can be done with minimal computational cost. Since the implementation is already in Python, extension to complex variable types to use the complex step derivative method is straight forward. The cross-sectional properties of the beam elements are generated from the spar geometry shown in Figure 5. The position and width of the spar can be varied as a design variable. The spar box is then defined with an additional thickness variable, offset towards the center, which determines the cross-sectional properties.

C. Aerostructural Analysis

The current work focuses strictly on the analysis and optimization of wind turbine blades. Two of the most significant disciplines are the aerodynamics and structures. It is common practice to use the aerodynamic forces to perform structural analysis. This however, doesn't strictly constitute a proper aerostructural analysis. A sound analysis is only possible when the structural deformation is returned to the aerodynamics and the coupled solution converged. The types of structural displacements that affect the aerodynamics are: the twist distribution, the coning angle distribution, and in general, the change in blade length due to both bending and centrifugal forces.

A number of techniques have been developed to satisfy the inter-disciplinary coupling. The multidisci-

plinary design feasible (MDF)[13] approach is adopted for this problem. A simple fixed point iteration scheme is used to ensure a multidisciplinary feasible solution at each iteration.

III. Turbine Blade Design Optimization

A. Optimization Algorithm

There is a wide variety of optimization algorithms that can be used to perform design optimization of engineering systems. These algorithms fit into one of two main categories: gradient-based methods and gradient-free methods. Gradient-free methods include genetic algorithms, the Nelder–Mead simplex, and particle swarm optimization (PSO).[14,15]

Gradient based algorithms use function gradients, and, depending on the method, can form second order information as well. Typical examples of gradient-based methods include the conjugate gradient method, the method of feasible descent (MFD), and sequential quadratic programming (SQP).

The results herein where optimized using SNOPT,[16] an optimizer based on the SQP approach. A gradient-based optimizer was chosen due to its greater suitability for solving problems with large numbers of design variables.

B. Sensitivity Analysis

Accurate sensitivity analysis is critical to the successful application of a gradient-based method to an optimization problem. The easiest sensitivity method to implement is first order forward (or backward) differencing. With careful selection of the step size, h, adequate accuracy using finite differencing methods can be accomplished. However, there is no guarantee the best step size at one design point will remain optimal as the solution progresses.

The complex step method[17] is a good alternative to finite-difference methods. If the computation involves calculations strictly in the real domain, the gradient can be approximated to second order by:

$$\frac{\mathrm{d}f(x)}{\mathrm{d}x} = \frac{\mathrm{Im}\left[f(x+ih)\right]}{h} + \mathcal{O}(h^2) \tag{16}$$

.

One major advantage of this approximation is that, unlike finite differences, it is not subject to subtractive cancellation errors for small step sizes. This allows the use of step size, h, *below* machine precision, generally of order 10^{-20}. For small enough h, the $\mathcal{O}(h^2)$ can be lower than machine zero and thus the approximation becomes numerically exact. To use this method, the analysis codes may have to be modified to accept complex arguments.

C. Objective Function

The choice of an objective function is not always an easy task and has a significant impact on the success of an optimization process. In general, the end goal of a wind turbine designer is to reduce the overall cost of energy (COE), defined as,

$$\mathrm{COE} = \frac{C}{\mathrm{AEP}} \tag{17}$$

where C is the total cost that accounts for materials, fabrication, transportation, construction and maintenance costs. AEP is the annual energy production. Typically COE is expressed in cents/kWh. The ability to simulate directly, and optimize for, the actual COE requires accurate knowledge of the cost breakdown just mentioned. Since this work is concerned strictly with the design of turbine blades, an alternative objective is used. If we maintain a fixed cost and maximize the AEP, this is equivalent to reducing the COE. Therefore the AEP (or equivalently the average turbine output power) is chosen as the objective to maximize while constraining particular aspects of the blade design that adversely affect the cost. The purpose of this objective is to simulate the re-design of the blades to take advantage of site-specific winds while maintaining compatibility with the the remainder of the wind turbine.

D. Design Variables

Seven groups of design variables are considered for this optimization: chord, twist, spar thickness, spar location, spar length, airfoil thickness, and rotation rate. The chord distribution determines the overall shape and area of the blade and we assume the blades have zero sweep angle and are tapered about the 1/4 chord position. The twist angle, θ in Figure 1, is the angle of the blades relative to the plane of rotation. The other design variables are the location of the center of the spar box from the leading edge (x_{spar}), the spar box length (L_{spar}) and the thickness of the spar walls (t_{spar}). The variables are defined only a limited number of radial positions to reduce the complexity of the problem. Cubic spline interpolation is utilized for interpolating the twist distribution while linear interpolation is utilized for the remainder of the design variable groups. An additional design variable, t_{foil}, represents the maximum thickness of the airfoil. Finally at each wind velocity the angular velocity may vary. This introduces an additional design variable for each velocity that is analyzed. The design variables for blade cross-section are shown in Figure 5.

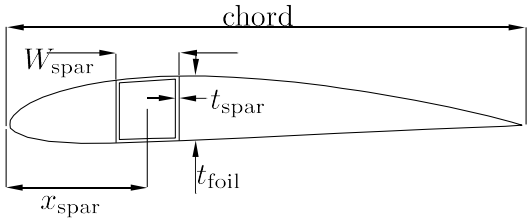

Figure 5. Design variable parameterization of an airfoil

E. Constraints

Most engineering optimization problems are constrained to ensure physically realizable designs. The constraints for this problem are as follows.

Von Mises Stresses: These are compute for each element in the structural model, at each velocity analyzed in the time-spectrum. While the material's yield stress might seem be a suitable upper bound, this ignores the fatigue effects that play an important role in the lifetime analysis of wind turbine blades. Thus, a maximum stress limit that is less than the yield stres is enforced.

Cost: Two measures are used to approximate the cost of the blade: spar mass and surface area. The upper bound for these quantities is set to the values given by the baseline design. Hence, the cost of the optimized blade should be very similar to that of the baseline design.

Maximum Power: This constraint is required to ensure the amount of shaft power transmitted to the generator does not exceed its maximum capacity.

F. Wind Velocity Profiles

The Canadian Wind Energy Atlas[18] produces computationally-derived wind speed data for the entire country. An example of this data for two specific locations are shown in figure 6. The two sites are chosen to represent the two differing types of environment where wind turbines may be expected to operate: a suburban environment with low to moderate wind resources (University of Toronto Institute for Aerospace Studies — UTIAS) and a commercial wind farm site[19] with high-quality wind resources (St. Lawrence, Newfoundland). The wind energy atlas provides histograms of the percentage of time the wind blows at each speed. This allows for the direct simulation of the total amount of mechanical output of the turbine and the ability to optimize designs to best match a particular distribution.

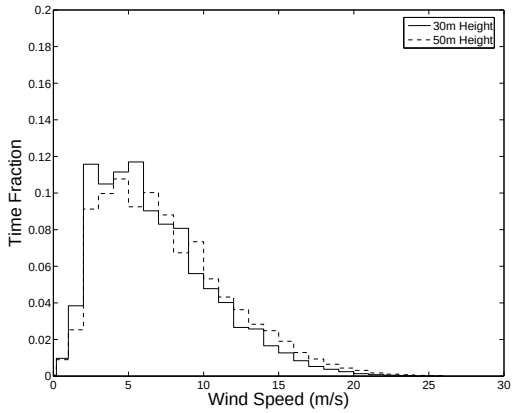

(a) Wind profile for St. Lawrence

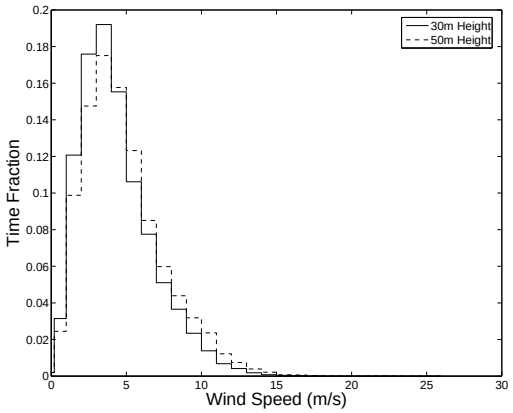

(b) Wind profile for UTIAS

Figure 6. Wind velocity profile data for two locations

IV. Results

A. Baseline Design

An existing commercial wind turbine, the Wes5 Tulipo ,[20] was chosen as the baseline design to demonstrate the capability of the wind turbine optimization framework. This is a small, 3 blade, fixed pitched, stall controlled, "urban" wind turbine with a rotor diameter of 5m and a maximum generator capacity of 5kW.

The starting point in the design space can have a significant impact on the optimization's outcome as it determines to which local optimum the optimizer will converge. In order to facilitate the optimization we choose an good baseline design. An estimate of the actual chord distribution for the Wes5 Tulip was deduced from technical drawings. We assume that the blades must be connected to a hub through a circular connection with a diameter no greater than 3". The remainder of the design variables required for the optimization were estimated. As a reasonable estimate of the twist distribution, we assumed an optimum axial induction factor of 1/3. Then,

$$\theta = \arctan\left(\frac{(2/3)V_{\text{design}}}{r\Omega_{\text{design}}}\right) - \bar{\alpha} \tag{18}$$

where $\bar{\alpha}$ is constant, design angle of attack, and r is the undeformed radius. For this example, V_{design} =9m/s, Ω_{design} =12rad/s and $\bar{\alpha}$ =12°. For the structural design, the position of the spar remained fixed at 30% of the chord. The initial spar length is set to 15% for the airfoil section and to 90% for the hub connection. A tapered thickness distribution is chosen that satisfies the stress constraints at the initial operating condition. The airfoils are initialized with a 0.16c thickness at the root and a 0.1c thickness at the tip. The rotor is designed to spin at a variable speed up to a maximum of 140rpm (14.7rad/s). The rotation rates correspond to a tip speed ratio of 6, as long as this does not exceed the design variable bounds. Note that the diameter of the rotor is fixed throughout the optimization. Upper and lower bounds of the design variables are shown in Table 1. Plots showing the initial condition in relation to the optimized results are shown in Figure 7.

B. Constraints

The specific values of the constraint limits are now explained. A fatigue limit of 40MPa for an aluminum alloy is enforced.[21] The surface area constraint of 0.83m^2 is computed directly from the approximate chord distribution of the baseline blade design. A maximum spar mass of 3.7kg is stipulated as the mass required to satisfy the stress constraints of the baseline design. This is consistent with overall trends noted by Hau.[21] An upper bound on the power of 5000W is enforced to match the maximum generator capacity. The geometric constraints make sure that the wall thickness of the spar structure does not produce a self-intersecting

Design Variable	Count	Lower Limit	Upper Limit
Chord	4	.05 m	.40 m
Twists	4	-75°	75°
W_{spar}	4	4%	30%
t_{spar}	4	0.3 mm	10mm
t_{foil}	3	6%	20%
Ω	varies (12)	7.5 rad/s	14.7 rad/s

Table 1. Design variables and their bounds

volume. A minimum gap of 0.5mm is stipulated. The constraints and their bounds are summarized in Table 2.

Constraint	Minimum	Maximum
Stress	-	40MPa
Spar Mass	-	3.7kg
Surface Area	-	0.83m^2
Power	-	5000 W
Geometry	0.5mm	-

Table 2. Optimization constraints

C. Optimized Wind Turbine Blades

Two optimizations are performed to determine the effect of the site-specific wind histogram on the optimized design. A multidisciplinary analysis is carried out at each of 12 wind velocities ranging from 4 to 20m/s, to determine the average power output (or equivalently, the annual energy production). Two locations, St. Lawrence, NL, and the location of the University of Toronto Institute for Aerospace Studies (UTIAS) are used for comparison. The average wind speeds for the two locations are 7.28m/s and 4.83m/s respectively, as calculated at a 30m reference height. The optimizations are run on a 2.4GHz Core2 Duo dekstop PC with the Linux OS Ubuntu 8.04. Each requires approximately 30 minutes to reduce the magnitude of the gradient by three orders of magnitude. At each of the optimum points, all constraints are satisfied. In both cases, the weight and surface area constraints are active, as well as a maximum stress constraint. Power is limited only on the two highest velocities for the St. Lawrence distribution. Figure 7 shows the baseline design, as well as the two optimal designs. The twist distributions are similar to the baseline. However, there are considerable variations: The optimized chord distributions, for example, are similar to each other, but considerably different from the baseline. The spar thickness distribution for each case is nearly the same. The airfoil thickness distribution for the UTIAS turbine shows a thicker tip profile and and reduced midsection thickness when compared to the St. Lawrence design.

Figure 8 demonstrates clearly the effect of the site-specific application. The design for the low wind potential site tries to maximize the power capture at the low range of velocities, from 4 to 9m/s, as these are the most prevalent. The high wind potential site foregoes the low wind potential and produces much higher power at speeds ranging from 9 to 20m/s.

Figures 9 to 12 show the resulting optimized blade shape. The blade surfaces are coloured with the BEM predicted axial induction factor and the internal spar structure is contoured with the von-Mises stress. The floating outline shows the aero-structurally displaced surface. At the 7m/s velocity, axial induction factors are approximately 0.25-0.3 and the structural stress is approximately 1/2 of the limit. At 12 m/s we see a significantly reduced axial induction factor and a nearly fully stressed spar structure.

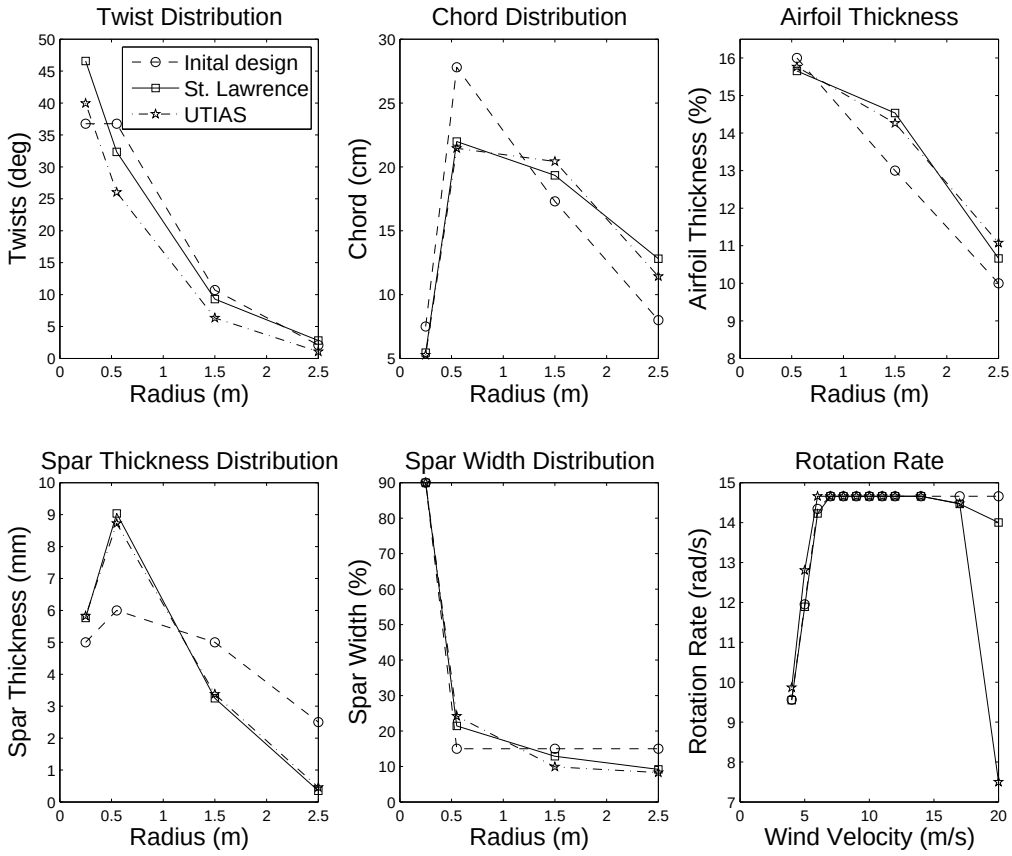

Figure 7. Design variable comparison of optimization results

Table 3 shows the results of each of the optimization. Despite a reasonably good baseline design, the optimizer increases the average output of each of the turbines by 26.7% and 29.2% respectively. However, more importantly, when the optimum turbine design from each location is analyzed in the alternate location, a 3 to 4% decrease in average power is observed. This shows the increases that may be expected for a cost-constrained turbine blade optimization optimization problem.

Location	$\bar{P}_{\text{init}}$ (W)	$\bar{P}_{\text{opt}}$ (W)	$\bar{P}_{\text{other-opt}}$ (W)	Site-specific increase
St. Lawrence	1566.1	1984.5	1905.1	4.17%
UTIAS	660.2	853.3	826.0	3.31%

Table 3. Average power of optimized wind turbines

V. Conclusions

This paper presents a multidisciplinary optimization framework for the design of wind turbine rotors. Aerodynamic modelling is achieved through a BEM method coupled with a structural model consisting of space beam finite elements. An SQP optimizer with gradients supplied by the complex-step method is used to perform the design optimization of the turbine blades. The objective was to maximize the wind

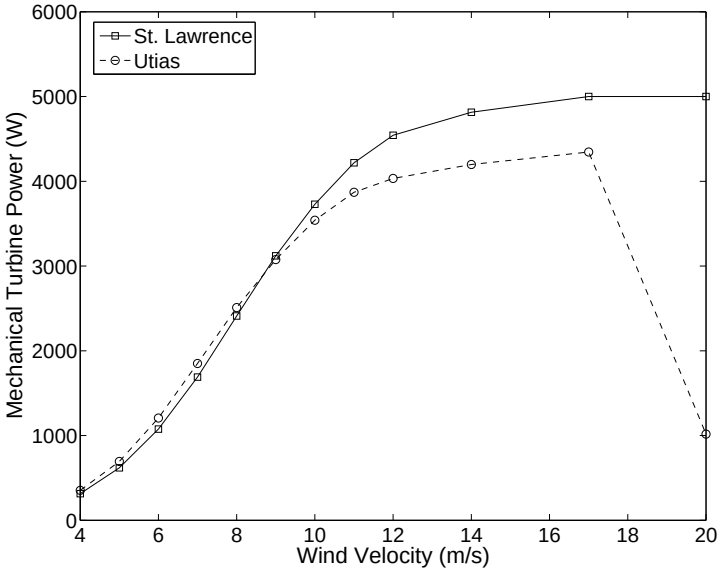

Figure 8. Power comparison of the two locations

turbine power output by changing the blade geometry and structural sizes, while maintaining a fixed cost and compatibility with the remainder of turbine system. A 5kW wind turbine test case was used to demonstrate the potential for site-specific optimizations. The framework presented enables turbine blade aerostructural optimization with modest shape dependencies. The ability to simulate the average power expected from specific localized wind distributions allows for detailed site-specific optimization. Optimization results for a small fixed pitch 5kW turbine indicate optimal design depends on the wind distribution. The optimization results for two specific locations indicate it is possible to achieve output increases of 3-4% compared to the optimal design for the other location. Future improvements and additions to the architecture are discussed that may increase the overall modelling accuracy as well as the suitability of potential solutions.

VI. Future Work

The results that have been presented in this paper do not fully exploit the potential of this optimization framework. Numerous areas of improvement have been identified to further the goals of this wind turbine optimization project.

A. Detailed Shape Optimization

The airfoil shape is controlled only by a single thickness parameter: the thickness parameter in the NACA 4-digit airfoil definition. While this introduces a variable that can take advantage of the trade-off between the structural stiffness and aerodynamic performance, it does not allow for precise control of the actual airfoil shape to exploit further aerostructural trade offs. The ability to parameterize airfoil shapes using cubic B-spline curves and to compute sensitivity information using a complex version of XFOIL has been developed, but no results are available yet. The application of these shape variables greatly increases the complexity of the design problem, since the aerodynamic data cannot be pre-computed and must be generated on demand. Regenerating a new set of α-Re maps for each function evaluation is not particularly costly, but considerable computational cost is added when a new map must be generated for each shape variable perturbation due to the sensitivity analysis. Investigation of methods that can be used to reduce this computational expense are being investigated.

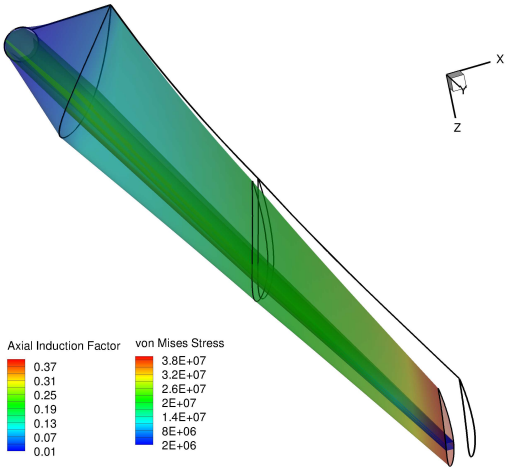

Figure 9. St. Lawrence optimized blade at 7m/s

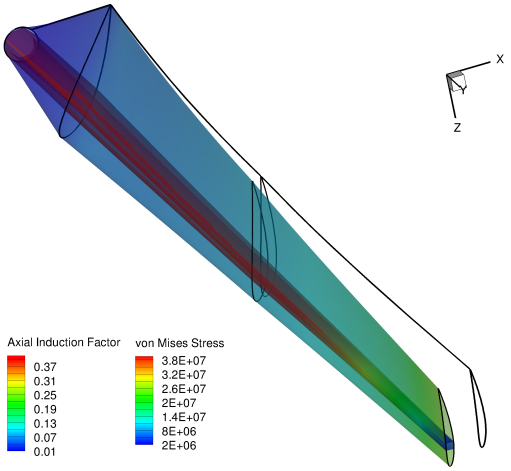

Figure 10. St. Lawrence optimized blade at 12m/s

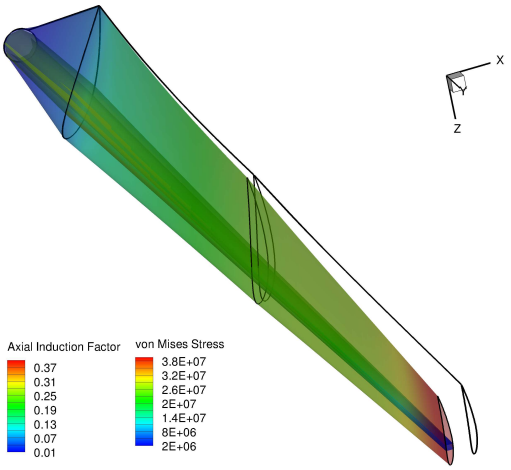

Figure 11. UTIAS optimized blade at 7m/s

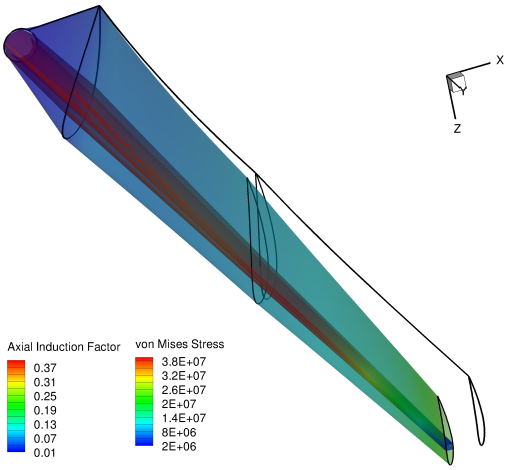

Figure 12. UTIAS optimized blade at 12m/s

B. Additional Analysis

The optimization results presented only aim to maximize the amount of mechanical power available to the generator. This ignores other disciplines which are required for a complete analysis. For example, this work does not consider the remainder of the turbine's electrical system or the cost associated with the turbine construction, installation, and maintenance. In addition, a time-dependant aero-structural simulation would provide an indication of the load frequency distribution allowing a more detailed fatigue analysis of the blades.

C. Analytic Sensitivity Methods

With an increase in the number of design variables, analytic sensitivity methods become attractive since the cost of sensitivity analysis can be made independent of the number of design variables. A coupled adjoint sensitivity method[22] could be applied to the current problem. The disadvantage of such adjoint methods is the time required for the sensitivity calculation is now proportional to the the number of output variables. This may cause problems since we have a large number of stress constraints. Methods for aggregating constraints, such as the Kreisselmeier–Steinhauser (KS) function could potentially be used.

D. Parallelization

No section of the analysis is currently computed in parallel. However, there are several instances where an embarrassingly parallel approach could be used. The BEM calculation of the axial and tangential induction factors for each section can be computed in parallel without knowledge of the remaining sections. Additionally, the analysis at each selected velocity bin is also an embarrassingly parallel task. Finally, the entire analysis procedure is easy to parallelize for use in gradient-free optimizations.

VII. Acknowledgements

We wish to thank Mr. Peter Jansen for generously supplying the structural code pyFEA to be used in this work. We are indebted to the Canada Research Chairs program and the Natural Sciences and Engineering Research Council for the provided funding.

References

[1]P. Fuglsang, C. Bak, J. G. Schepers, B. Bulder, T. T. Cockerill, P. Claiden, A. Olesen, R. van Rossen, "Site-specific Design Optimization of Wind Turbines," *Wind Energy*, Vol. 5, 2002, pp. 261–279.

[2]Fuglsang, P., "Site-Specific Design Optimization of 1.5-2.0 MW Wind Turbines," *Trnasactions of the ASME*, Vol. 123, 2201, pp. 296–303.

[3]Benini, E., "Optimal Design of Horizontal-Axis Wind Turbines Using Blade-Element Theory and Evolutionary Computation," *Journal of Solar Energy Engineering*, Vol. 124, 2002, pp. 357–363.

[4]J. Méndez, D. G., "Wind blade chord and twist angle optimization using genetic algoritms," *Fifth International Conference on Engineering Computational Technology*, Las Palmas de Gran Canaria, Spain,, September 2006.

[5]Fuglsang, P. and Madsen, H., "Optimization Method for Wind Turbine Rotors," *Journal of Wind Engineering and Industrial Aerodynamics*, Vol. 80, 1999, pp. 191–206.

[6]Drela, M., "XFOIL — An analysis and design system for low Reynolds number airfoils," *Low Reynolds number aerodynamics*, Notre Dame,Germany, Federal Republic of, 5-7 June 1989.

[7]Peterson, P., Martins, J. R. R. A., and Alonso, J. J., "Fortran to Python Interface Generator with an Application to Aerospace Engineering," *Proceedings of the 9th International Python Conference, Long Beach, CA*, 2001.

[8]Hansen, M. O., *Aerodynamics of Wind Turbines*, James & James (Science Publishers) Ltd., 35-37 William Road, London, 2000.

[9]R. Mikkelsen, J. N. S. and Shen, W. Z., "Modelling and Analysis of the Flow Field around a Coned Rotor," *Wind Energy*, Vol. 4, 2001, pp. 121–135.

[10]National Institute of Standards and Technology, "Package CMLIB," Internet, http://gams.nist.gov/serve.cgi/Package/CMLIB/.

[11]Tangler, J. and Kocurek, J. D., "Wind Turbine Post-Stall Airfoil Performance Characteristics Guidelines for Blade-Element Momentum Methods," *43rd AIAA Aerospace Sciences Meeting and Exhibit*, Reno, Nevada, 10-13 January 2005.

[12]Montgomerie, B., "Method for root effect, tip effects and extending the angle of attack range to $\pm$ 180°, with application to aerodynamics for blades on wind turbines and propellers," Scientific Report ISSN 1650-1942, Swedish Defence Research Agency, SE-172 90 Stockholm, June 2004.

[13]Cramer, E. J., Dennis, J. E., Frank, P. D., Lewis, R. M., and Shubin, G. R., "Problem formulation for multidisciplinary optimization," *SIAM Journal on Optimization*, Vol. 4, 1994, pp. 754–776.

[14]Perez, R. and Behdinan, K., "Particle Swarm Approach for Structural Design Optimization," *International Journal of Computer and Structures*, Vol. 85, No. 19-20, October 2007, pp. 1579–1588.

[15]Perez, R. and Behdinan, K., *Swarm Intelligence: Focus on Ant and Particle Swarm Optimization*, chap. Particle Swarm Optimization in Structural Design, International Journal of Advanced Robotic Systems, 1st ed., September 2007, pp. 373–394, ISBN 978-3-902613-09-7.

[16]Gill, P. E., Murray, W., and Saunders, M. A., "SNOPT: An SQP Algorithm for Large-Scale Constrained Optimization," *SIAM Review*, Vol. 47, No. 1, 2005, pp. 99–131.

[17]Martins, J. R. R. A., Sturdza, P., and Alonso, J. J., "The Complex-Step Derivative Approximation," *ACM Transactions on Mathematical Software*, Vol. 29, No. 3, 2003, pp. 245–262.

[18]Environment-Canada, "Canadian Wind Energy Atlas," Website, October 2006, http://www.windatlas.ca/.

[19]Herridge, P., "Final turbine erected at St. Lawrence wind farm," The Southern Gazette (Newspaper), July 2008.

[20]Solutions, W. E., "Wes5 Tulipo," Internet, http://www.windenergysolutions.nl/wes5/index.htm, 2005.

[21]Hau, E., *Wind Turbines- Fundamentals, Technologies, Application, Economics*, Springer, 2nd ed., 2006.

[22]Martins, J. R. R. A., Alonso, J. J., and Reuther, J. J., "A Coupled-Adjoint Sensitivity Analysis Method for High-Fidelity Aero-Structural Design," *Optimization and Engineering*, Vol. 6, No. 1, March 2005, pp. 33–62.

[23]Larrabee, E. and French, S., "Minimum induced loss windmills and propellers," *Journal of Wind Engineering and Industrial Aerodynamics*, Vol. 15, 1983, pp. 317–327.

[24]Crawford, C., "Re-examining the Precepts of the Blade Element Momentum Theory for Coning Rotors," *Wind Energy*, Vol. 9, 2006, pp. 457–478.